

ENHANCED PHOTOMETRY USING STEREPHOTOCLINOMETRY ON THE MOON. E. E. Palmer^{1*} and D. L. Domingue¹, *epalmer@psi.edu, ¹Planetary Science Institute, 1700 E. Fort Lowell, Suite 106, Tucson AZ, 85719, USA.

Introduction: Photometric characterization of a planetary surface is highly dependent on the accuracy to which the illumination and viewing conditions can be determined. Due to the difficulties of registering imaging data to a high-resolution digital terrain model (DEM), photometric analyses typically neglect the effect of local topography, and instead uses global values. We have developed a technique that allows us to integrate local topography (on meter scales) into the photometric analysis of the lunar surface. Photometric characterization of the lunar surface is the first step in a process to generate a thermal correction for the Moon Mineralogy Mapper (M³) data, which will improve the detection of water on the Moon [1 – 6] and its correlation with such surface properties as slope, roughness, and composition.

Stereophotoclinometry: The first step for incorporating the illumination (incidence angle) and viewing (emission angle) geometries from local topography into photometric analyses is to develop an ultra-high resolution terrain model of the surface. Using Lunar Reconnaissance Orbiter Camera (LROC) data, we have constructed a DEM for Tsiolkovsky crater using the techniques of stereophotoclinometry (SPC) [7]. We selected a specific sub-region that includes several types of terrains and a variety of slopes and slope orientations. The test region contains the mare floor of the crater, a rill within the mare, and one of the andesitic uplifts from the central peak. There are substantial variations in the terrain slope orientations within this test region, including south-facing slopes that will have lower temperatures due to their lower insolation. The source LROC data has a resolution of 0.5 meters, while the DEM has a grid spacing of 1.5 meters with a vertical precision of approximately 1 meter. The test region is a 2,000 x 2,000 pixel region with 5 meter pixels (i.e. 10 km x 10 km).

Photometric Cubes: The next step in this topographically-enhanced photometric analysis is the construction of “Photometric Cubes”. Photometric cubes are layered images, in which each layer contains specific data relevant to the pixel position within the cube. For each LROC image that falls within our test region we generate a 4-band cube where the four layers contain the reflectance (I/F), phase angle (α), incidence angle (i), and emission angle (e). The I/F values come directly from the calibrated LRO NAC images themselves. The phase angle is generated from the United States Geologic Survey (USGS) Integrated Software

for Imagers and Spectrometers (ISIS) tool. Incidence and emission angles are calculated directly from the topographic model using the spacecraft and sun positions. The NAC images are narrower than our test region, so multiple images are required to fully mosaic the selected area. Figure 1 shows the parameters derived from image M110751047RC.

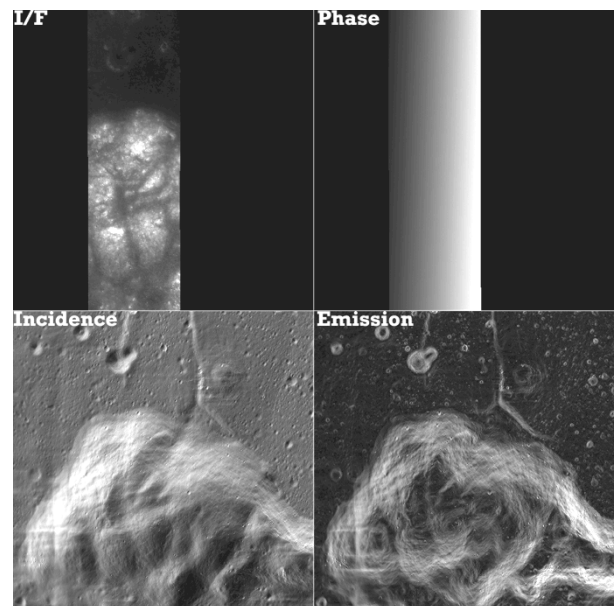


Figure 1. The 4 bands from the photometric cube constructed for LROC image M110751047RC. The incidence band (bottom left) and emission band (bottom right) are derived from the DEM, and thus show the values for these angle over the entire test region. The I/F band (top left) and the phase angle band (top right) are derived from the image and only display the values for the regions imaged within the test area registered to their physical location within the test region.

The key component to generating the photometric cubes is the registration process performed by SPC. We use SPC to identify several thousand control-points (a.k.a. landmarks) in an image that locks its position to the existing DEM and registers it at a 1/10th of a pixel accuracy. Once this is performed on all the images, any location within the working region (2,000 x 2,000 pixel) can be selected and the exact I/F for each observation of that surface feature, along with the associated α , i , and e can be retrieved.

Grouping: While this technique would enable you to perform photometric analyses on a pixel-by-pixel basis, the number of images acquired by LROC is limited, requiring grouping of pixels. We used the full resolution LROC images to define several categories of terrains. By grouping similar terrains, a single image no longer provides a single data point for a phase function for photometric modeling (i.e. average I/F , α , i , and e), but provides a much larger set of data (Fig. 2). Here the phase changes little across the image field of view, but the range of incidence and emission angles is significant.

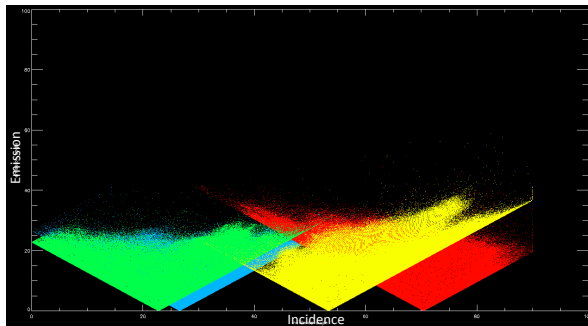


Figure 2. Plot of incidence versus emission angle values across the maria floor portion of the test region in Tsiolkovsky crater. These angle values were extracted from the four images used in the preliminary analyses (blue: M110751047RC, red: M103668324L, green: M123730396L, yellow: M103675484L)

Photometric Characterization Strategy: The photometric data extracted from the Tsiolkovsky crater test region is being partitioned based on geologic unit and regolith morphology. The partitions begin with two basic divisions: crater floor maria and central peak uplift. Each of these two regions are to be photometrically modeled individually. These regions are then to be further divided. The floor maria units will include: (1) crater and crater ejecta, (2) rill, and (3) boulder regions. The central peak uplift units will include: (1) crater and crater ejecta, (2) boulder regions, and (3) sloped walls (further divided by orientation: north-, south-, east-, and west-facing).

Each surface unit will be modeled using Hapke's model [8 – 14], which is based on geometric optics and the equations of radiative transfer, and a second model described by Kaasalainen et al. [15] and Shkuratov et al. [16], which has been recently applied to Vesta [17], the Moon [16], and Mercury [18] (hereafter referred to as the Kaasalainen-Shkuratov model). The Kaasalainen-Shkuratov model separates the effects due to phase angle (the angle between the incident and

reflected rays of light) from those due to incidence and emission angles (which are measured from the surface normal and thus depend on local topography). The results from each model will be used to derive and compare the Bond albedo for the different regolith region divisions, which in turn provides a surface temperature and thermal spectrum.

Preliminary Results: Hapke modeling of the floor maria (large crater, rill, and boulder fields excluded) has been performed. A preliminary Bond albedo of 0.063 was derived for of this region, based on a phase integral value of 0.458 and physical albedo of 0.137 calculated from the modeling results.

References: [1] Vilas, F. et al. 2008. *Earth Planets Space* 60, 67. [2] Clark, R.N., 2009. *Science* 326, 562. [3] Pieters, C. M., et al. 2009. *Science* 326, 568. [4] Sunshine, J. M., et al. 2009. *Science* 326, 565. [5] McCord, T. B., et al. 2011. *J. Geophys. Res.* 106, 3311. [6] Clark et al. 2011. LPI Contribution #1621, p8. [7] Gaskell R. W. (2008) *Meteoritics & Planet. Sci.* 43, 1049-1062. [8] Hapke, B., 1981. *J. Geophys. Res.* 68, 4571-4586. [9] Hapke, B., 1984. *Icarus* 59, 41-59. [10] Hapke, B., 1986. *Icarus* 67, 264-280. [11] Hapke, B., 1993. *Theory of Reflectance and Emittance Spectroscopy*. Cambridge University Press, N.Y., 455 pp. [12] Hapke, B., 2002. *Icarus* 157, 523-534. [13] Hapke, B., 2008. *Icarus* 195, 918-926. [14] Hapke, B., 2012. *Theory of Reflectance and Emittance Spectroscopy*. Cambridge University Press, N.Y., 2nd Ed., 513 pp. [15] Kaasalainen, M., et al., 2001. *Icarus* 153, 37-51. [16] Shkuratov Y., et al., 2011. *Planet. Space Sci.* 59, 1326-1371. [17] Schröder, S.E., et al., 2013. *Planet. Space Sci.* 85, 198-213. [18] Domingue, D.L. et al. 2015, 46th LPSC, abstract 1341, this meeting.

Acknowledgement: This work was supported by NASA grant NNX13AJ63G under the LASER program.